

Instanton Effects in QCD at High Baryon Density

T. Schäfer^{1,2,3}

¹*Department of Physics, Duke University, Durham, NC 27708*

²*Department of Physics, SUNY Stony Brook, Stony Brook, NY 11794*

³*Riken-BNL Research Center, Brookhaven National Laboratory, Upton, NY 11973*

Abstract

We study instanton effects in QCD at very high baryon density. In this regime instantons are suppressed by a large power of (Λ_{QCD}/μ) , where Λ_{QCD} is the QCD scale parameter and μ is the baryon chemical potential. Instantons are nevertheless important because they contribute to several physical observables that vanish to all orders in perturbative QCD. We study, in particular, the chiral condensate and its contribution $m_{GB}^2 \sim m\langle\bar{\psi}\psi\rangle$ to the masses of Goldstone bosons in the CFL phase of QCD with $N_f = 3$ flavors. We find that at densities $\rho \sim (5 - 10)\rho_0$, where ρ_0 is the density of nuclear matter, the result is dominated by large instantons and subject to considerable uncertainties. We suggest that these uncertainties can be addressed using lattice calculations of the instanton density and the pseudoscalar diquark mass in QCD with two colors. We study the topological susceptibility and Witten-Veneziano type mass relations in both $N_c = 2$ and $N_c = 3$ QCD.

I. INTRODUCTION

Strange quark matter at very high baryon density but low temperature is believed to be in the color-flavor-locked (CFL) phase [1–3]. The CFL phase is characterized by diquark condensates which break both the global $SU(3)_L \times SU(3)_R$ flavor symmetry and the local $SU(3)$ color symmetry but preserve a global $SU(3)_V$. In addition to that, diquark condensation spontaneously breaks the exact $U(1)_V$ and approximate $U(1)_A$ symmetry of QCD. The low energy behavior of the CFL phase is governed by the corresponding Goldstone bosons, an octet of pseudoscalar mesons associated with chiral symmetry breaking and two singlets associated with the breaking of $U(1)_{V,A}$.

The CFL phase has many similarities with $N_f = 3$ QCD at low density [1,4], but the mechanism of chiral symmetry breaking is quite different. In particular, if the baryon density is very large, the dominant order parameter for chiral symmetry breaking is not the usual quark-anti-quark condensate $\langle \bar{\psi}\psi \rangle$, but a four-fermion operator $\langle (\bar{\psi}\psi)^2 \rangle \sim \langle \psi\psi \rangle^2$. As a consequence, the masses squared of the pseudoscalar Goldstone bosons are quadratic, not linear, in the quark masses. The coefficient of proportionality can be computed in perturbative QCD [5–12].

The CFL diquark condensate leaves a discrete axial $(Z_2)_A$ symmetry unbroken. Since the quark-anti-quark condensate is odd under this symmetry, $\langle \bar{\psi}\psi \rangle$ remains zero in weak coupling perturbation theory. Non-perturbative effects, instantons, break the $(Z_2)_A$ symmetry and lead to a non-zero expectation value $\langle \bar{\psi}\psi \rangle$. If the density is large instantons are strongly suppressed and $\langle \bar{\psi}\psi \rangle$ is small. As the density decreases instantons become more important and the chiral condensate grows. Our main objective in the present work is to compute the linear term in the mass relation for the Goldstone bosons. The relative size of the linear and quadratic terms in the mass relation provides an estimate of the baryon density at which the crossover from the asymptotic regime, in which chiral symmetry breaking is dominated by the diquark condensate, to the low density regime, in which chiral symmetry breaking is governed by the quark-anti-quark condensate, occurs.

The size of the linear term in the Goldstone boson mass relation also has important consequences for the phase structure of CFL matter in the presence of a non-zero strange quark mass and lepton chemical potentials [13–19]. Bedaque and Schäfer argued that for physical values of the quark masses and the baryon chemical potential CFL quark matter is likely to be kaon condensed [17]. This conclusion was based on an analysis of the effective potential for the chiral order parameter. The low energy constants that appear in the effective potential were obtained in perturbation theory, but the conclusions are unchanged if the coefficients are estimated using dimensional analysis. This suggests that the results of the perturbative calculation are qualitatively correct even in the regime of strong coupling. However, the assumption that instanton effects are small for the densities of interest is crucial.

The paper is organized as follows. In section II we compute the instanton contribution to Goldstone boson masses in the CFL phase. In section III we study corrections to this result due to the finite size of instantons. In section IV we compute the pseudoscalar diquark mass in QCD with two colors. This observable can be studied with present lattice techniques. We also comment on Witten-Veneziano relations in QCD at high baryon density. Our results extend previous work in [20,2,8,21].

II. INSTANTON CONTRIBUTION TO CFL CHIRAL THEORY

In this section we consider the CFL phase of high density quark matter. For excitation energies smaller than the gap the only relevant degrees of freedom are the Goldstone modes associated with the breaking of chiral symmetry and baryon number. The interaction of the Goldstone modes is described by the effective Lagrangian [22]

$$\begin{aligned}
\mathcal{L}_{eff} = & \frac{f_\pi^2}{4} \text{Tr} \left[\nabla_0 \Sigma \nabla_0 \Sigma^\dagger - v_\pi^2 \partial_i \Sigma \partial_i \Sigma^\dagger \right] + \frac{3f^2}{4} \left[\partial_0 V \partial_0 V^* - v_{\eta'}^2 \partial_i V \partial_i V^* \right] \\
& + \left[A \text{Tr}(M \Sigma^\dagger) V^* + h.c. \right] \\
& + \left[B_1 \text{Tr}(M \Sigma^\dagger) \text{Tr}(M \Sigma^\dagger) V + B_2 \text{Tr}(M \Sigma^\dagger M \Sigma^\dagger) V + B_3 \text{Tr}(M \Sigma^\dagger) \text{Tr}(M^\dagger \Sigma) + h.c. \right] + \dots
\end{aligned} \tag{1}$$

Here $\Sigma = \exp(i\phi^a \lambda^a / f_\pi)$ is the chiral field, f_π and f are the octet and singlet decay constants, M is a complex mass matrix. The chiral field and the mass matrix transform as $\Sigma \rightarrow L\Sigma R^\dagger$ and $M \rightarrow LMR^\dagger$ under chiral transformations $(L, R) \in SU(3)_L \times SU(3)_R$. The axial $U(1)_A$ field is $V = \exp(i\phi) = \exp(2i\eta' / (\sqrt{6}f))$. As explained in [17] the covariant derivative $\nabla_0 \Sigma$ contains the effective chemical potentials $X_L = (MM^\dagger)/(2\mu)$ and $X_R = (M^\dagger M)/(2\mu)$,

$$\nabla_0 \Sigma = \partial_0 \Sigma + i \left(\frac{MM^\dagger}{2\mu} \right) \Sigma - i \Sigma \left(\frac{M^\dagger M}{2\mu} \right). \quad (2)$$

The coefficients B_i of the quadratic mass terms were computed in [5–12] by matching the mass dependence of the vacuum energy computed in perturbative QCD and the CFL chiral theory. The result is [5,12]

$$B_1 = -B_2 = \frac{3\Delta^2}{4\pi^2}, \quad B_3 = 0, \quad (3)$$

where Δ is the gap in the quasi-particle spectrum. We shall determine the coefficient A by computing the shift in the vacuum energy linear in the quark mass. This shift is due to the first order instanton contribution to the vacuum energy in the background of a perturbatively generated diquark condensate, see the diagram shown in Fig. 1a. In QCD with three flavors, the instanton induced interaction between quarks is given by [23–25]

$$\begin{aligned} \mathcal{L} = \int n(\rho, \mu) d\rho & \frac{(2\pi\rho)^6 \rho^3}{6N_c(N_c^2 - 1)} \epsilon_{f_1 f_2 f_3} \epsilon_{g_1 g_2 g_3} \left(\frac{2N_c + 1}{2N_c + 4} (\bar{\psi}_{R,f_1} \psi_{L,g_1}) (\bar{\psi}_{R,f_2} \psi_{L,g_2}) (\bar{\psi}_{R,f_3} \psi_{L,g_3}) \right) \\ & - \frac{3}{8(N_c + 2)} (\bar{\psi}_{R,f_1} \psi_{L,g_1}) (\bar{\psi}_{R,f_2} \sigma_{\mu\nu} \psi_{L,g_2}) (\bar{\psi}_{R,f_3} \sigma_{\mu\nu} \psi_{L,g_3}) + (L \leftrightarrow R). \end{aligned} \quad (4)$$

Here, ρ is the instanton size, μ is the quark chemical potential, f_i, g_i are flavor indices and $\sigma_{\mu\nu} = \frac{i}{2}[\gamma_\mu, \gamma_\nu]$. The instanton size distribution $n(\rho, \mu)$ is given by

$$n(\rho, \mu) = C_N \left(\frac{8\pi^2}{g^2} \right)^{2N_c} \rho^{-5} \exp \left[-\frac{8\pi^2}{g(\rho)^2} \right] \exp \left[-N_f \rho^2 \mu^2 \right], \quad (5)$$

$$C_N = \frac{0.466 \exp(-1.679N_c) 1.34^{N_f}}{(N_c - 1)!(N_c - 2)!}, \quad (6)$$

$$\frac{8\pi^2}{g^2(\rho)} = -b \log(\rho\Lambda), \quad b = \frac{11}{3}N_c - \frac{2}{3}N_f. \quad (7)$$

At zero density, the ρ integral in equ. (5) is divergent at large ρ . This is the well-known infrared problem of the semi-classical approximation in QCD. At large chemical potential,

however, large instantons are suppressed and the typical instanton size is $\rho \sim \mu^{-1} \ll \Lambda^{-1}$.

To linear order in the quark mass one of the three zero modes is lifted. We obtain

$$\begin{aligned} \mathcal{L} = \int n(\rho, \mu) d\rho \frac{2(2\pi\rho)^4 \rho^3}{4(N_c^2 - 1)} \epsilon_{f_1 f_2 f_3} \epsilon_{g_1 g_2 g_3} M_{f_3 g_3} & \left(\frac{2N_c - 1}{2N_c} (\bar{\psi}_{R, f_1} \psi_{L, g_1}) (\bar{\psi}_{R, f_2} \psi_{L, g_2}) \right. \\ & \left. - \frac{1}{8N_c} (\bar{\psi}_{R, f_1} \sigma_{\mu\nu} \psi_{L, g_1}) (\bar{\psi}_{R, f_2} \sigma_{\mu\nu} \psi_{L, g_2}) + (M \leftrightarrow M^\dagger, L \leftrightarrow R) \right), \end{aligned} \quad (8)$$

We can now compute the expectation value of equ. (8) in the CFL ground state [2,20,21].

Using the perturbative result for the diquark condensate in the CFL phase,

$$\begin{aligned} \langle \psi_{L, f}^a C \psi_{L, g}^b \rangle &= -\langle \psi_{R, f}^a C \psi_{R, g}^b \rangle = (\delta_f^a \delta_g^b - \delta_g^a \delta_f^b) \Phi, \\ \Phi &= \frac{3\sqrt{2}\pi}{g} \Delta \left(\frac{\mu^2}{2\pi^2} \right), \end{aligned} \quad (9)$$

we find the instanton contribution to the vacuum energy density

$$\mathcal{E} = - \int n(\rho, \mu) d\rho \frac{16}{3} (\pi\rho)^4 \rho^3 \left[\frac{3\sqrt{2}\pi}{g} \Delta \left(\frac{\mu^2}{2\pi^2} \right) \right]^2 \text{Tr} [M + M^\dagger]. \quad (10)$$

We note that for $M = \text{diag}(m_u, m_d, m_s)$ the instanton contribution to the vacuum energy is indeed negative. Since the effective interaction involves both left and right-handed fermions the relative phase between the left and right-handed condensate in equ. (9) is important. Instantons favor the state with $\langle \psi_L \psi_L \rangle = -\langle \psi_R \psi_R \rangle$ which is the parity even ground state. Equation (10) for the vacuum energy can be matched against the effective lagrangian equ. (1). We find

$$A = C_N \frac{8\pi^4}{3} \frac{\Gamma(6)}{3^6} \left[\frac{3\sqrt{2}\pi}{g} \Delta \left(\frac{\mu^2}{2\pi^2} \right) \right]^2 \left(\frac{8\pi^2}{g^2} \right)^6 \left(\frac{\Lambda}{\mu} \right)^{12} \Lambda^{-3}, \quad (11)$$

where we have performed the integral over the instanton size ρ using the one-loop beta function. We note that A is related to the quark-anti-quark condensate, $\langle \bar{\psi} \psi \rangle = -2A$. Equation (11) agrees, up to a numerical factor and a power of g , with the estimate presented in [2,8]. We can also determine the masses of Goldstone bosons. We take into account the instanton contribution equ. (11), the $O(M^2)$ term given in equ. (3) and the $O(M^4)$ term given in equ. (2). To this order, the masses of the charged Goldstone bosons are given by

$$\begin{aligned}
m_{\pi^\pm} &= \mp \frac{m_d^2 - m_u^2}{2\mu} + \left[\frac{2A}{f_\pi^2}(m_u + m_d) + \frac{4B}{f_\pi^2}(m_u + m_d)m_s \right]^{1/2}, \\
m_{K^\pm} &= \mp \frac{m_s^2 - m_u^2}{2\mu} + \left[\frac{2A}{f_\pi^2}(m_u + m_s) + \frac{4B}{f_\pi^2}m_d(m_u + m_s) \right]^{1/2}, \\
m_{K^0, \bar{K}^0} &= \mp \frac{m_s^2 - m_d^2}{2\mu} + \left[\frac{2A}{f_\pi^2}(m_d + m_s) + \frac{4B}{f_\pi^2}m_u(m_d + m_s) \right]^{1/2}.
\end{aligned} \tag{12}$$

In the flavor symmetric limit $m_u = m_d = m_s \equiv m$ the one-instanton contribution to the mass of the η' is

$$m_{\eta'}^2 = \frac{4A}{f^2}m. \tag{13}$$

If flavor symmetry is broken the η' mixes with the η and π^0 [8,10,12]. We note that at the one-instanton level, the mass of the η' vanishes in the chiral limit. The η' -mass in the chiral limit arises from the two-instanton diagrams shown in Figs. 1c)-1e). These diagrams are hard to evaluate and we will not pursue this problem here. However, even without a calculation we can determine the dependence of the instanton generated potential on the QCD theta angle θ and the $U(1)_A$ phase ϕ of the chiral field. Again restricting ourselves to the case of exact flavor symmetry we find

$$V = -6mA \cos(\theta + \phi) - 12m^2B \cos(\phi) - 2C \cos(2\theta + 3\phi), \tag{14}$$

where A is the coefficient of the one-instanton contribution given in equ. (11), $B = B_1 = B_2$ is the coefficient of the $O(M^2)$ term given in equ. (3), and C is the coefficient of the two-instanton term. The potential equ. (14) determines the topological susceptibility in the CFL phase. In the limit of very small quark masses we find

$$\chi_{top} = \frac{2mA}{3} = -\frac{m\langle\bar{\psi}\psi\rangle}{3}. \tag{15}$$

This result agrees with prediction of anomalous Ward identities at zero density. If we take the chemical potential to infinity while keeping the quark mass fixed then $m^2B \gg mA \gg C$ and the topological susceptibility is given by $\chi_{top} = 6mA = -3m\langle\bar{\psi}\psi\rangle$.

In the following, we will study the mass of the K^0 in more detail. The mass of the K^0 receives the largest instanton contribution and is of special interest in connection with

kaon condensation. Different contributions to the K^0 -mass are shown in Fig. 2. The $O(m)$ and $O(m^2)$ contributions are computed from equ. (12) taking into account only the terms proportional to A and B , respectively. The $O(m^4)$ term $(m_s^2 - m_d^2)/(2\mu)$ increases the mass of the \bar{K}^0 , but decreases the mass of the K_0 . The complete result for the K^0 mass is shown in Fig. 3. If the $O(m^4)$ term is bigger than the $O(m, m^2)$ contribution then K^0 condensation takes place and the mass of the K^0 vanishes. We have used $m_u = 4$ MeV, $m_d = 7$ MeV, $m_s = 150$ MeV and the perturbative result for the gap [26–29]

$$\Delta = 512\pi^4 2^{-1/3} (2/3)^{-5/2} b'_0 \mu g^{-5} \exp\left(-\frac{3\pi^2}{\sqrt{2}g}\right), \quad (16)$$

where b'_0 is a constant which is determined by non-Fermi liquid effects [30,31] that are not included in our calculation. To leading order in perturbation theory the pion decay constant is given by [5,10,32,33]

$$f_\pi^2 = \frac{21 - 8 \log(2)}{18} \left(\frac{\mu^2}{2\pi^2}\right). \quad (17)$$

Qualitatively, the instanton contribution to the kaon mass scales as

$$m_K|_{inst} \sim \left(\frac{m_s}{\Lambda}\right)^{1/2} \left(\frac{\Delta}{\Lambda}\right) \left(\frac{\Lambda}{\mu}\right)^5 \left[\log\left(\frac{\mu}{\Lambda}\right)\right]^{7/2} \Lambda. \quad (18)$$

This shows that the result is strongly suppressed as $\mu \rightarrow \infty$. We also note, however, that the result is quite sensitive to the value of the scale parameter Λ . In practice, the power dependence on the scale parameter is canceled to some degree by the logarithmic dependence. This can be seen from the results shown in Fig. 2. At $\mu = 500$ MeV, the instanton contribution to m_{K^0} calculated from equ. (11) varies between 85 MeV and 120 MeV if the scale parameter is varied between 180 MeV and 280 MeV.

The dependence of m_{K^0} on the scale parameter provides a naive estimate of the importance of higher order corrections. In the present case this is probably an underestimate. This can be seen by studying the role of higher order corrections in the instanton size distribution. At two-loop order we have

$$n_{II}(\rho, \mu) = C_N (\beta_I(\rho))^{2N_c} \rho^{-5} \exp\left[-\beta_{II}(\rho) - N_f \rho^2 \mu^2\right], \quad (19)$$

$$\beta_I(\rho) = -b \log(\rho\Lambda), \quad b = \frac{11}{3}N_c - \frac{2}{3}N_f, \quad (20)$$

$$\beta_{II}(\rho) = \beta_I(\rho) + \frac{b'}{2b} \log\left(\frac{2\beta_I(\rho)}{b}\right), \quad b' = \frac{34}{3}N_c^2 - \frac{13}{3}N_fN_c + \frac{N_f}{N_c}. \quad (21)$$

The instanton contribution to the kaon mass calculated with the two-loop instanton distribution is also shown in Fig. 2. We observe that the results are significantly smaller as compared to the leading order estimate. We find $m_{K^0}(inst) = (17 - 40)$ MeV compared to the leading order result $m_{K^0}(inst) = (85 - 120)$ MeV. The large difference between the one and two-loop results is related to the fact that at moderate density perturbation theory predicts that the average instanton size is not small. Using equns. (5,10) we get

$$\bar{\rho} = \frac{\Gamma(13/2)}{\Gamma(6)} (\sqrt{3}\mu)^{-1} \simeq 1.4\mu^{-1}. \quad (22)$$

For $\mu = 500$ MeV we find $\bar{\rho} = 0.55$ fm, which is bigger than the standard estimate for the typical instanton size at zero density $\bar{\rho}_0 = (0.3 - 0.4)$ fm. The situation is somewhat improved for the two-loop size distribution which gives $\bar{\rho} = 0.45$ fm. The main difference between the one and two-loop size distributions is that at two-loop order the pre-exponent is evaluated at a scale given by the inverse instanton size ρ^{-1} rather than at the external scale μ . This difference is formally of higher order, but at moderate density it provides a significant suppression of large instantons.

We can also study this problem in a different way. It is clear that at small density there has to be some non-perturbative effect that eliminates the contribution of large-size instantons. We can simulate this effect in terms of a non-perturbative screening factor $\exp(-\rho^2 m_{scr}^2)$ in the instanton size distribution. If the screening mass is adjusted in such a way that the average instanton size at $\mu = 500$ MeV is equal to the phenomenological value at $\mu = 0$, $\bar{\rho} = 0.35$ fm, then we find $m_{K^0}(inst) = (7 - 12)$ MeV.

The sensitivity of the instanton contribution to the kaon mass to large-size instantons translates into a large uncertainty regarding the behavior of kaons at finite density. If large instantons with $\rho \simeq 0.5$ fm play a role then the kaon mass is dominated by the instanton contribution and kaon condensation is unlikely. If the typical instanton size satisfies $\rho <$

0.35 fm then the instanton contribution to the kaon mass is at most comparable to the perturbative contribution and kaon condensation is likely.

III. FINITE INSTANTON SIZE EFFECTS

In the previous section we computed the instanton contribution to the vacuum energy using the effective instanton induced interaction equ. (4). This effective interaction is derived under the assumption that the relevant momenta are smaller than the inverse instanton size, $p, \mu \ll \rho^{-1}$. In our case the relevant momenta are on the order of the Fermi momentum $|\vec{p}| \sim p_F \sim \mu$ and the typical instanton size is given by $\rho \sim \mu^{-1}$, so $p\rho \sim 1$. This implies that finite size effects are potentially important.

Instanton finite size effects can be determined from the fermion zero mode solution at finite baryon density. This solution was found in [34] and studied in [35,20,36]. Using the exact zero mode solution amounts to the replacement

$$\bar{\psi}_{f\alpha i} \rightarrow \frac{1}{2\pi} \bar{\psi}_{f\alpha j} \mathcal{F}_i^j, \quad \psi^{f\alpha i} \rightarrow \frac{1}{2\pi} \mathcal{F}_j^{\dagger i} \psi^{f\alpha j} \quad (23)$$

in the effective interaction equ. (4). Here, the instanton form factors $\mathcal{F}, \mathcal{F}^\dagger$ are given by [20,36]

$$\mathcal{F}_i^j = [(\tilde{p} \cdot \sigma^-)(\varphi \cdot \sigma^+)]_i^j, \quad \mathcal{F}_j^{\dagger i} = [(\varphi^* \cdot \sigma^-)(\tilde{p} \cdot \sigma^+)]_j^i \quad (24)$$

with $\sigma_\mu^\pm = (\pm i\vec{\sigma}, 1)$, $\tilde{p} = (\vec{p}, p_4 + i\mu)$, $\varphi_\alpha = \varphi_\alpha(p, \mu)$ and $\varphi_\alpha^* = [\varphi_\alpha(p, -\mu)]^*$. The instanton form factors are determined by the Fourier transform $\varphi_\alpha(p, \mu)$ of the instanton zero mode wave function. For completeness, we provide the result for $\varphi_\alpha(p, \mu)$ in appendix A.

We first study how the instanton form factor modifies the loop integral which contains the mass insertion, see equ. (8). In this case we need the quark-anti-quark form factor

$$G_1(p) = \frac{1}{2(2\pi)^2} \delta_l^i \delta_k^j \mathcal{F}_i^k(p) \mathcal{F}_j^{\dagger l}(p). \quad (25)$$

We find $G_1(p) = (p + i\mu)^2 \varphi_\alpha(p, \mu) \varphi_\alpha(p, \mu) / (2\pi)^2$. We can now perform the loop integral with the mass insertion. We find

$$2N_c \int \frac{d^4p}{(2\pi)^4} \frac{mG_1(p)}{(p+i\mu)^2} = \frac{N_c m}{(2\pi\rho)^2}, \quad (26)$$

where we have used the normalization condition equ. (A6) for the Fourier transform of the zero mode wave function. We observe that the instanton form factor does not modify equ. (8).

The next step is the integration over the quark-quark propagators, equ. (10). The diquark loop involves the form factors

$$F_1(p) = \frac{1}{2(2\pi)^2} \epsilon^{ik} \mathcal{F}_i^j(p) \mathcal{F}_k^l(-p) \epsilon_{jl} \quad (27)$$

$$F_2(p) = \frac{1}{2(2\pi)^2} \epsilon^{ik} \mathcal{F}_i^j(p) \mathcal{F}_k^l(-p) \epsilon_{jm} [(\sigma_0)(\vec{\sigma} \cdot \hat{p})]_l^m. \quad (28)$$

These two structures arise from the contraction of the instanton vertex with the diquark propagator

$$S_{12}(p) = \frac{1}{2} (1 + \vec{\alpha} \cdot \hat{p}) C \gamma_5 \frac{\Delta(|\vec{p}|)}{p_4^2 + (|\vec{p}| - \mu)^2 + \Delta^2}. \quad (29)$$

The two form factors $F_{1,2}(p)$ are given by

$$F_1(p) = \frac{-1}{(2\pi)^2} \left\{ (p^2 + \mu^2) \varphi(p, \mu) \cdot \varphi(-p, \mu) + (p + i\mu) \cdot \varphi(p, \mu) (p - i\mu) \cdot \varphi(-p, \mu) \right. \\ \left. - (p + i\mu) \cdot \varphi(-p, \mu) (p - i\mu) \cdot \varphi(p, \mu) \right\}, \quad (30)$$

$$F_2(p) = \frac{i}{(2\pi)^2} \left\{ (p + i\mu) \cdot \varphi(p, \mu) \left[(p_4 - i\mu) \hat{p} \cdot \vec{\phi}(-p, \mu) - p \varphi_4(-p, \mu) \right] \right. \\ \left. - (p - i\mu) \cdot \varphi(-p, \mu) \left[(p_4 + i\mu) \hat{p} \cdot \vec{\phi}(p, \mu) - p \varphi_4(p, \mu) \right] \right\}. \quad (31)$$

The functions $F_{\pm}(p) = F_1(p) \pm F_2(p)$ are shown in Figs. 4,5. We observe that the form factors are centered around the Fermi surface, $p_4 = 0$, $|\vec{p}| = \mu$. This is an important observation. Instantons produce $(\bar{\psi}_R \psi_L)$ -particle-hole pairs near the Fermi surface, and the chirality violating pair creation amplitude is therefore not suppressed by Pauli-blocking [20]. In Fig. 4 we study the dependence of $F_{\pm}(p)$ on ρ at fixed baryon chemical potential μ . We find that on the Fermi surface $F_+ = 1$ for all ρ whereas $F_- \rightarrow 1$ only as $\rho \rightarrow 0$. In practice we are interested in the limit $\mu \rightarrow \infty$ with $\rho \sim \mu^{-1}$. This limit is studied in Fig. 5. Again we observe that $F_+(p=\mu, p_4=0) = 1$ for all μ .

In the weak coupling limit the contraction of the diquark propagator equ. (29) with the instanton vertex only involves the F_+ form factor. Expanding $F_+(p)$ around the Fermi surface and using $F_+(\mu, 0) = 1$ we can show that up to corrections of order $O(g^2)$ the instanton form factor does not modify the weak coupling result equ. (11) for A . In the same fashion we can also show that up to corrections of order $O(g^2)$ there is no anti-gap (F_-) contribution to A .

We have also studied the effect of the instanton form factor at moderate density. The integral over the diquark propagator is given by

$$\Phi = \int \frac{d^4p}{(2\pi)^4} \frac{F_+(p)\Delta(|\vec{p}|)}{p_4^2 + (|\vec{p}| - \mu)^2 + \Delta^2}. \quad (32)$$

For $F_+(p) = 1$ we recover the perturbative result equ. (9). Results for the kaon mass with the effects of the instanton form factor included are shown in Fig. 6. At a baryon chemical potential $\mu = 500$ MeV the instanton form factor leads to a modest reduction of the instanton contribution to the kaon mass on the order of 40%. This reduction is due to the fact that the instanton form factor suppresses the contribution from large instantons. This effect, however, does not lead to a significant reduction of the average instanton size. In particular, the discrepancy between the one and two-loop results remains large.

IV. QCD WITH TWO COLORS

Given the large uncertainty in the instanton contribution to the Goldstone boson masses at moderate baryon density it would clearly be useful if the result could be checked on the lattice. Because of the sign problem direct studies of $N_c = 3$ QCD are still not feasible. On the other hand, QCD with $N_c = 2$ colors and $N_f = 2$ flavors does not suffer from a sign problem at non-zero baryon density and has been studied successfully on the lattice [38–40].

In QCD with two colors we also expect the formation of a diquark condensate at large baryon density [37]. For $N_f = 2$ flavors the diquark condensate breaks the $U(1)_B$ of baryon number and the anomalous $U(1)_A$ symmetry, but not the $SU(2)_L \times SU(2)_R$ chiral symmetry.

The $U(1)_B$ Goldstone boson is exactly massless, but the $U(1)_A$ Goldstone boson acquires a mass from instantons. The corresponding contribution to the vacuum energy is shown in Fig. 1f. Except for the mass insertion, the diagram is identical to the $O(m)$ contribution to the vacuum energy in the CFL phase of $N_c = N_f = 3$ QCD.

The effective lagrangian for the pseudoscalar Goldstone boson is

$$\mathcal{L} = \frac{f^2}{2} [(\partial_0\phi)^2 - v^2(\partial_i\phi)^2] - V(\phi). \quad (33)$$

We can think of ϕ as the relative phase between the left and right handed diquark condensate. Since baryon number is broken, the field ϕ has the quantum numbers of both pseudoscalar mesons and diquarks. This means that the mass of the ϕ -field governs the asymptotic behavior of both the η' and pseudoscalar diquark correlation functions. The decay constant f and Goldstone boson velocity v can be determined in perturbation theory. The result is identical to the one in QCD with $N_c = 3$ colors and $N_f = 2$ flavors [5,10]

$$f^2 = \left(\frac{\mu^2}{4\pi^2}\right), \quad v^2 = \frac{1}{3}. \quad (34)$$

The potential $V(\phi)$ is determined by instantons. The calculation of the instanton induced potential is completely analogous to the case $N_c = 3, N_f = 2$ [21], so we can be brief here. We find $V(\phi) = A_2 \cos(\phi - \theta)$ where θ is the QCD theta angle and

$$A_2 = C_N 8\pi^4 \left[\frac{4\pi}{g} \Delta \left(\frac{\mu^2}{2\pi^2} \right) \right]^2 \left(\frac{8\pi^2}{g^2} \right)^4 \left(\frac{\Lambda}{\mu} \right)^8 \Lambda^{-2}. \quad (35)$$

In $N_c = 2$ QCD the gap Δ is given by

$$\Delta = 512\pi^4 b'_0 \mu g^{-5} \exp\left(-\frac{2\pi^2}{g}\right). \quad (36)$$

Using these results we can determine the mass of the pseudoscalar Goldstone boson. We find

$$m_\phi^2 = \frac{A_2}{f^2}. \quad (37)$$

This result looks like the Witten-Veneziano relation [41,42]

$$m_{\eta'}^2 = \frac{2N_f \chi_{top}}{f_{\eta'}^2}, \quad (38)$$

where A_2 plays the role of the topological susceptibility¹. We note, however, that the topological susceptibility vanishes in the chiral limit, $\chi_{top} = O(m^2)$. Indeed, A_2 is not the topological susceptibility but the density of instantons, $A_2 = (N/V)$. This is consistent with the idea that in a dilute system of instantons local fluctuations of the topological charge are Poissonian. This means that $\chi_{top}(V) = \langle Q^2 \rangle / V = (N/V)$ for any 4-volume V which is large compared to the average volume per instanton and small compared to the screening volume [43,25],

$$(N/V)^{-1} \ll V \ll r_D^4, \quad (39)$$

where $r_D \sim m_{\eta'}^{-1}$ is the screening length. Because of the large mass of the η' this window does not exist in QCD at zero density. In QCD at asymptotically high baryon density the decay constant scales as the baryon chemical potential, $f \sim \mu$, the η' mass is much smaller than $(N/V)^{1/4}$, and the window described by equ. (39) opens up [21].

Mass relations of the Witten-Veneziano type can also be derived in QCD with $N_c = 3$ colors. The case of $N_f = 2$ flavors is exactly analogous to the $N_c = N_f = 2$ case except that the numerical value of the finite volume susceptibility $\chi_{top}(V)$ is different [21]. In the $N_f = 3$ CFL phase we also find that the η' -mass in the chiral limit satisfies a finite-volume Witten-Veneziano relation, $m_{\eta'}^2 f_{\eta'}^2 = 6\chi_{top}(V)$. In this case, however, we have $\chi_{top}(V) = 2(N/V)$ because instantons occur in pairs.

We can also study how the relation between the η' mass and the topological susceptibility is modified if quark masses are included. In the regime in which the η' mass is dominated by the linear mass term, equ. (13), we find $m_{\eta'}^2 f_{\eta'}^2 = (4/9)\chi_{top}(V)$. In this regime the topological

¹The extra factor $2N_f$ is related to our normalization of f . If we define $f_{\eta'}$ in such a way that the canonical axial current $A_0 = \bar{\psi}\gamma_0\gamma_5\frac{\tau_0}{2}\psi$ is represented in the effective theory by $A_0 = f_{\eta'}\partial_0\eta' + \dots$ then we find $m_{\eta'}^2 f_{\eta'}^2 = 4A_2$.

charge is only partially screened, $\chi_{top}(V \rightarrow \infty) = \frac{1}{9}\chi_{top}(V)$. If the quark mass is even larger and the quadratic mass term dominates the relation between the η' mass and the topological susceptibility is lost.

In Figs. 7,8 we show numerical results for the η' mass and the instanton density in QCD with $N_c = N_f = 2$. We again find that at moderate densities, $\mu \simeq 500$ MeV, the result is dominated by relatively large instantons $\bar{\rho} \simeq 0.5$ fm. The one-loop results for both the η' mass and the instanton density are surprisingly large. Both are bigger than the phenomenological values $m_{\eta'} = 945$ MeV and $(N/V) \simeq 1 \text{ fm}^{-4}$ in $N_c = 3$ QCD at zero baryon density. This is incompatible with the idea that $m_{\eta'}$ and (N/V) decrease as a function of density, and that the dependence on N_c is weak. Lattice simulations of $N_c = 2$ also point to a very light pseudoscalar diquark [39,40]. We should note, however, that these simulations were performed with more than two continuum quark flavors.

V. SUMMARY

We have computed the instanton contribution to the masses of Goldstone bosons in the CFL phase of QCD with three quark flavors. Our main result is given in equns. (11) and (12). At very large baryon density this result is expected to be exact.

At densities $\rho \simeq (5 - 10)\rho_0$ that are of interest in connection with the physics of neutron stars the perturbative result is very sensitive to the contribution of large instantons. For $\mu = 500$ MeV leading order perturbation theory predicts $\bar{\rho} = 0.55$ fm and $m_K(inst) = (85 - 120)$ MeV. If this result is reliable, then instantons would almost certainly prevent kaon condensation in the CFL phase at densities $\rho < 10\rho_0$. The situation is different if the two-loop instanton size distribution is used. In this case we find $\bar{\rho} = 0.45$ fm and $m_K(inst) = (17 - 40)$ MeV. The result is further reduced if a phenomenological screening mass and the instanton form factor is taken into account. In this case we find $m_K(inst) = (7 - 12)$ MeV.

We suggest that these uncertainties can be addressed using lattice calculations of the instanton density and the pseudoscalar diquark mass in $N_c = 2$ QCD. The result of the

leading order calculation, equ. (38) suggests that the pseudoscalar diquark mass is much bigger than 2Δ . This prediction is only weakly dependent on the value of the scale parameter and the magnitude of the gap Δ . We also emphasize that the pseudoscalar diquark mass is related to the topological susceptibility in a finite volume.

Acknowledgments: We would like to thank M. Alford, P. Bedaque, G. Carter, C. Manuel, D. Son, and M. Stephanov for useful discussions. This work was supported in part by US DOE grant DE-FG-88ER40388.

APPENDIX A: FOURIER TRANSFORM OF FERMION ZERO MODES

We repeat the results for the Fourier transform of the fermion zero mode wave function [20,36]. We follow the notation of [36]. The Fourier transform is given by

$$\psi_{L,R}(p, \mu)^{\alpha i} = \varphi_\nu(p, \mu) \left(\sigma_\nu^\pm \right)_j^i \epsilon^{jk} U_k^\alpha. \quad (\text{A1})$$

The temporal and spatial components of φ_ν are given by

$$\varphi_4(p_4, p, \mu) = \frac{\pi \rho^2}{4p} \left\{ (p - \mu - ip_4) [(2p_4 + i\mu) f_{1-} + i(p - \mu - ip_4) f_{2-}] \right. \\ \left. + (p + \mu + ip_4) [(2p_4 + i\mu) f_{1+} - i(p + \mu + ip_4) f_{2+}] \right\}, \quad (\text{A2})$$

$$\vec{\varphi}(p_4, p, \mu) = \frac{\pi \rho^2 \hat{p}_i}{4p} \left\{ (2p - \mu) (p - \mu - ip_4) f_{1-} + (2p + \mu) (p + \mu + ip_4) f_{1+} \right. \\ \left. + \left(2(p - \mu) (p - \mu - ip_4) - \frac{1}{p} (\mu + ip_4) [p_4^2 + (p - \mu)^2] \right) f_{2-} \right. \\ \left. + \left(2(p + \mu) (p + \mu + ip_4) + \frac{1}{p} (\mu + ip_4) [p_4^2 + (p + \mu)^2] \right) f_{2+} \right\} \quad (\text{A3})$$

where $p = |\vec{p}|$, $\hat{p} = \vec{p}/p$ and we have introduced the functions

$$f_{1\pm} = \frac{1}{z_\pm} [I_1(z_\pm) K_0(z_\pm) - I_0(z_\pm) K_1(z_\pm)], \quad (\text{A4})$$

$$f_{2\pm} = \frac{1}{z_\pm^2} I_1(z_\pm) K_1(z_\pm). \quad (\text{A5})$$

The argument of $f_{1,2\pm}$ is given by $z_\pm = \frac{1}{2}\rho\sqrt{p_4^2 + (p \pm \mu)^2}$. The Fourier transform $\varphi_\nu(p, \mu)$ satisfies the normalization condition

$$\int \frac{d^4 p}{(2\pi)^4} \varphi_\nu(p, \mu) \varphi_\nu(p, \mu) = \int \frac{d^4 p}{(2\pi)^4} [\varphi_\nu(p, -\mu)]^* \varphi_\nu(p, \mu) = \frac{1}{2\rho^2}. \quad (\text{A6})$$

REFERENCES

- [1] M. Alford, K. Rajagopal and F. Wilczek, Nucl. Phys. **B537**, 443 (1999) [hep-ph/9804403].
- [2] T. Schäfer, Nucl. Phys. **B575**, 269 (2000) [hep-ph/9909574].
- [3] N. Evans, J. Hormuzdiar, S. D. Hsu and M. Schwetz, Nucl. Phys. B **581**, 391 (2000) [hep-ph/9910313].
- [4] T. Schäfer and F. Wilczek, Phys. Rev. Lett. **82**, 3956 (1999) [hep-ph/9811473].
- [5] D. T. Son and M. Stephanov, Phys. Rev. **D61**, 074012 (2000) [hep-ph/9910491], erratum: hep-ph/0004095.
- [6] M. Rho, A. Wirzba, and I. Zahed, Phys. Lett. **B473**, 126 (2000) [hep-ph/9910550].
- [7] D. K. Hong, T. Lee, and D. Min, Phys. Lett. **B477**, 137 (2000) [hep-ph/9912531].
- [8] C. Manuel and M. H. Tytgat, Phys. Lett. **B479**, 190 (2000) [hep-ph/0001095].
- [9] M. Rho, E. Shuryak, A. Wirzba and I. Zahed, Nucl. Phys. A **676**, 273 (2000) [hep-ph/0001104].
- [10] S. R. Beane, P. F. Bedaque, and M. J. Savage, Phys. Lett. **B483**, 131 (2000) [hep-ph/0002209].
- [11] D. K. Hong, Phys. Rev. D **62**, 091501 (2000) [hep-ph/0006105].
- [12] T. Schäfer, Phys. Rev. **D**, in press, hep-ph/0109052.
- [13] M. Alford, J. Berges and K. Rajagopal, Nucl. Phys. **B558**, 219 (1999) [hep-ph/9903502].
- [14] T. Schäfer and F. Wilczek, Phys. Rev. **D60**, 074014 (1999) [hep-ph/9903503].
- [15] M. Alford, J. Bowers and K. Rajagopal, Phys. Rev. D **63**, 074016 (2001) [hep-ph/0008208].

- [16] T. Schäfer, Phys. Rev. Lett. **85**, 5531 (2000) [nucl-th/0007021].
- [17] P. F. Bedaque and T. Schäfer, Nucl. Phys. **A697**, 802 (2002) [hep-ph/0105150].
- [18] M. Alford, K. Rajagopal, S. Reddy and F. Wilczek, Phys. Rev. D **64**, 074017 (2001) [hep-ph/0105009].
- [19] D. B. Kaplan and S. Reddy, hep-ph/0107265.
- [20] R. Rapp, T. Schäfer, E. V. Shuryak, and M. Velkovsky, Annals Phys. **280**, 35 (2000), [hep-ph/9904353].
- [21] D. T. Son, M. A. Stephanov and A. R. Zhitnitsky, Phys. Lett. B **510**, 167 (2001) [hep-ph/0103099].
- [22] R. Casalbuoni and D. Gatto, Phys. Lett. **B464**, 111 (1999) [hep-ph/9908227].
- [23] G. 't Hooft, Phys. Rev. Lett. **37**, 8 (1976).
- [24] M. A. Shifman, A. I. Vainshtein and V. I. Zakharov, Nucl. Phys. B **163**, 46 (1980).
- [25] T. Schäfer and E. V. Shuryak, Rev. Mod. Phys. **70**, 323 (1998) [hep-ph/9610451].
- [26] D. T. Son, Phys. Rev. D **59**, 094019 (1999) [hep-ph/9812287].
- [27] T. Schäfer and F. Wilczek, Phys. Rev. **D60**, 114033 (1999) [hep-ph/9906512].
- [28] D. K. Hong, V. A. Miransky, I. A. Shovkovy and L. C. Wijewardhana, Phys. Rev. **D61**, 056001 (2000) [hep-ph/9906478].
- [29] R. D. Pisarski and D. H. Rischke, Phys. Rev. **D61**, 074017 (2000) [nucl-th/9910056].
- [30] W. E. Brown, J. T. Liu and H. Ren, Phys. Rev. **D61**, 114012 (2000) [hep-ph/9908248].
- [31] Q. Wang and D. H. Rischke, nucl-th/0110016.
- [32] K. Zarembo, Phys. Rev. D **62**, 054003 (2000) [hep-ph/0002123].
- [33] V. A. Miransky, I. A. Shovkovy and L. C. Wijewardhana, Phys. Rev. D **63**, 056005

- (2001) [hep-ph/0009173].
- [34] A. A. Abrikosov, *Yad. Fiz.* **37**, 772 (1983).
- [35] T. Schäfer, *Phys. Rev. D* **57**, 3950 (1998) [hep-ph/9708256].
- [36] G. W. Carter and D. I. Diakonov, *Nucl. Phys. A* **661**, 625 (1999), [hep-ph/9908314].
- [37] R. Rapp, T. Schäfer, E. V. Shuryak and M. Velkovsky, *Phys. Rev. Lett.* **81**, 53 (1998) [hep-ph/9711396].
- [38] E. Dagotto, F. Karsch and A. Moreo, *Phys. Lett. B* **169**, 421 (1986).
- [39] S. Hands, J. B. Kogut, M. P. Lombardo and S. E. Morrison, *Nucl. Phys. B* **558**, 327 (1999) [hep-lat/9902034].
- [40] J. B. Kogut, D. K. Sinclair, S. J. Hands and S. E. Morrison, *Phys. Rev. D* **64**, 094505 (2001) [hep-lat/0105026].
- [41] E. Witten, *Nucl. Phys. B* **156**, 269 (1979).
- [42] G. Veneziano, *Nucl. Phys. B* **159**, 213 (1979).
- [43] E. V. Shuryak and J. J. Verbaarschot, *Phys. Rev. D* **52**, 295 (1995) [hep-lat/9409020].

FIGURES

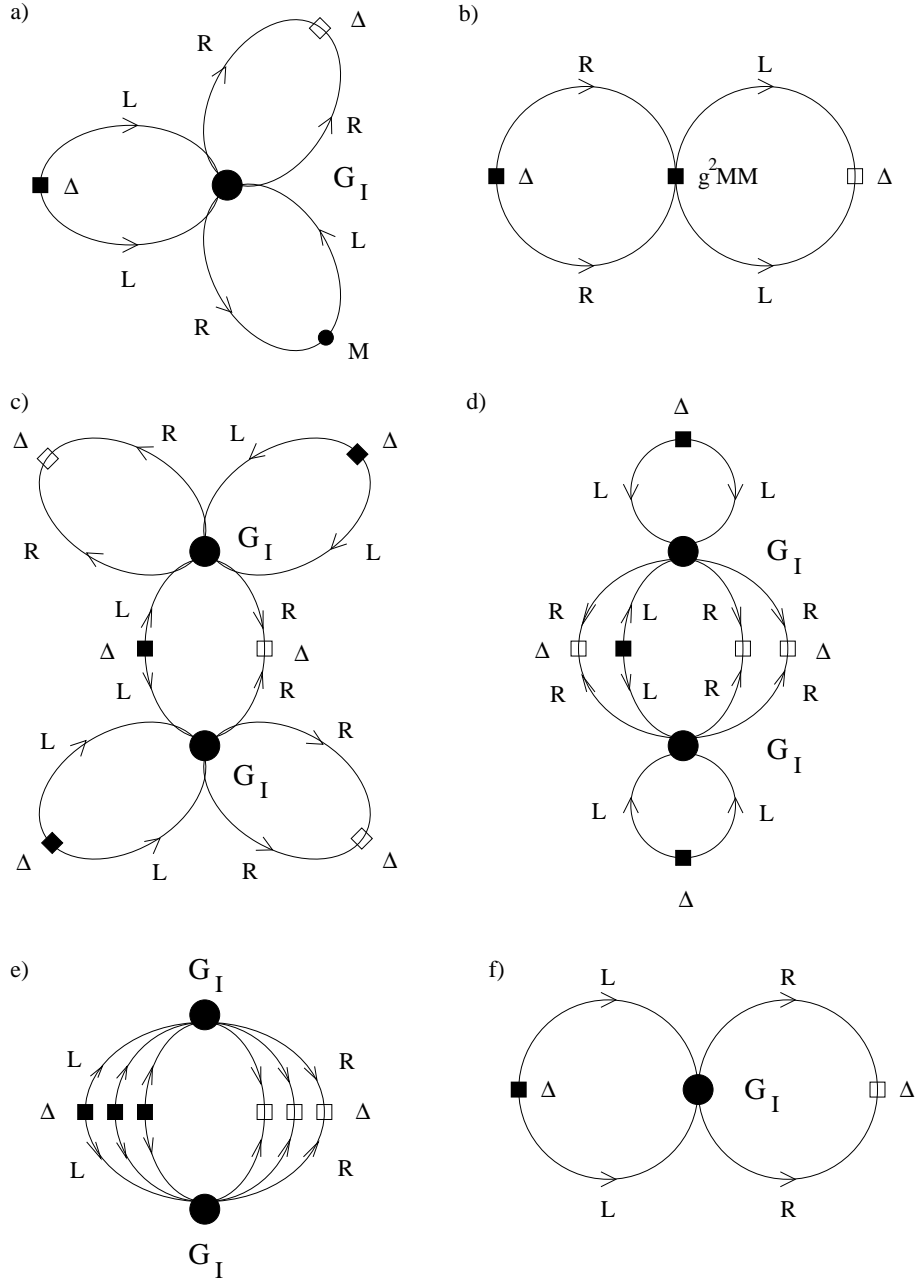


FIG. 1. Figure a) shows the $O(M)$ instanton contribution to the vacuum energy in the CFL phase. The six-fermion vertex is the effective 't Hooft vertex in the field of an instanton. Figure b) shows the $O(M^2)$ perturbative contribution to the vacuum energy. The four-fermion vertex corresponds to hard ($p \sim p_F$) electric gluon exchange. Figures c),d) and e) show the two-instanton contribution to the vacuum energy in the chiral limit. Figure f) shows the instanton contribution to the vacuum energy in QCD with two colors and two flavors.

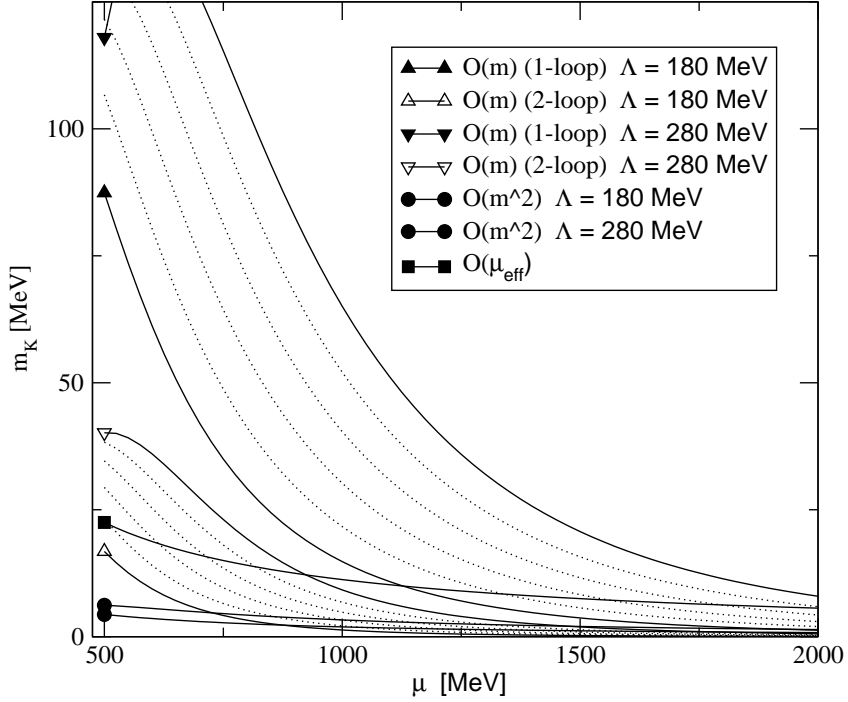


FIG. 2. Different contributions to the K^0 mass at finite baryon density. The two sets of dotted lines bounded by solid lines marked with triangles show the instanton contribution to the kaon mass computed for different values of the Λ parameter in the range $\Lambda = (180 - 280)$ MeV. The curves marked with solid (open) triangles are computed with the one-loop (two-loop) instanton distribution. The solid lines marked with circles show the perturbative $O(m^2)$ contribution for two different values of the scale parameter. The solid line marked by a square shows the absolute magnitude of the effective chemical potential $O(\mu_{\text{eff}}^2) = O(m^4)$ contribution.

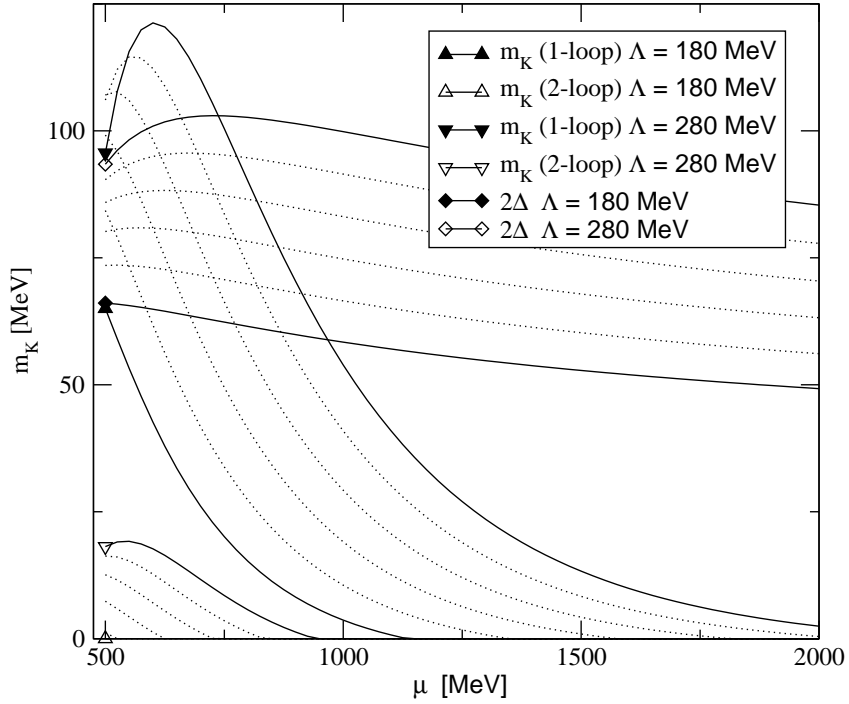


FIG. 3. This figure shows the sum of the different contributions to the K^0 mass shown in Fig. 2. For comparison we also show the gap 2Δ in the excitation spectrum for different values of the scale parameter in the range $\Lambda = (180 - 280)$ MeV.

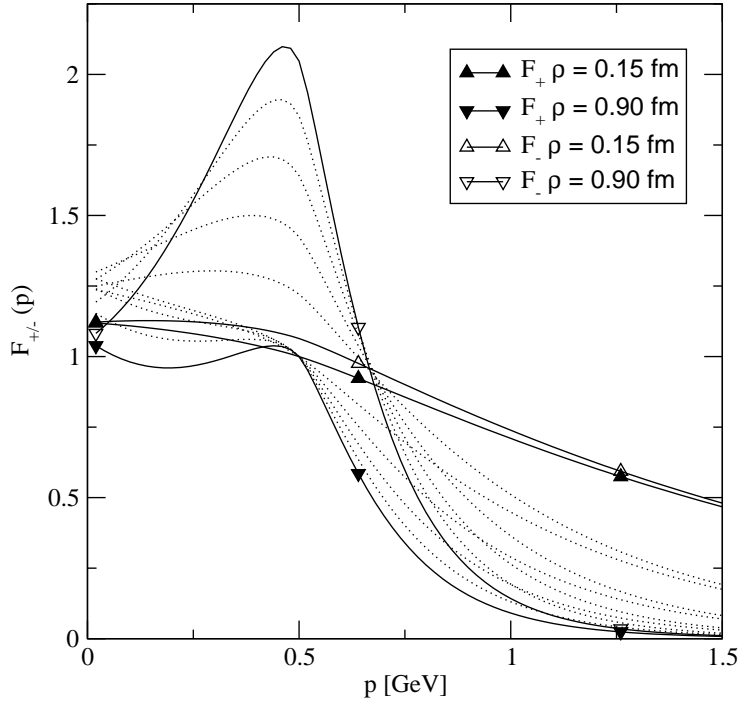


FIG. 4. Instanton form factors F_{\pm} for quark-quark scattering. The form factors are shown as a function of $p = |\vec{p}|$ for $p_4 = 0$. The Fermi momentum was chosen to be $p_F = 0.5$ GeV. The different curves correspond to instanton sizes in the range $\rho = (0.15 - 0.90)$ fm.

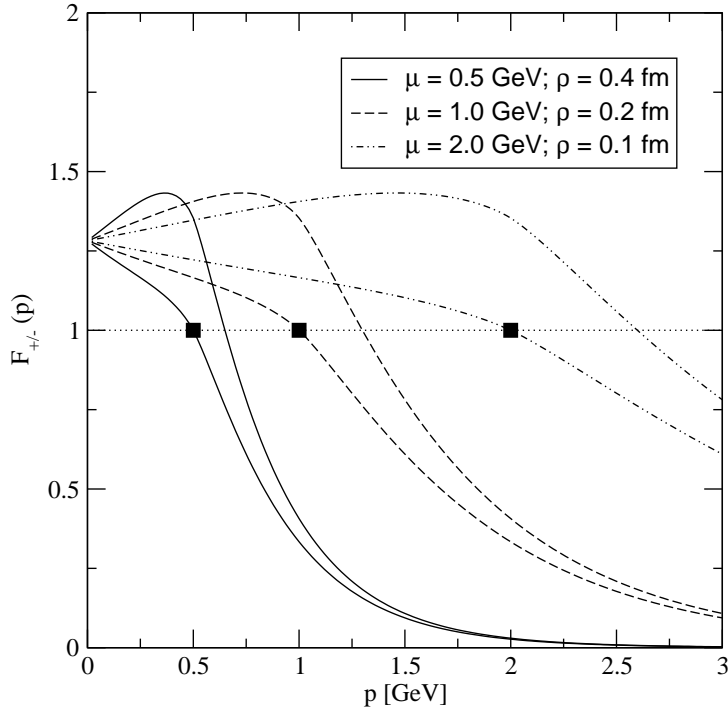


FIG. 5. Same as Fig. 4 for different Fermi momenta $p_F = 0.5, 1.0, 2.0$ GeV. The upper and lower curves show F_- and F_+ , respectively. The solid square shows the value of F_+ on the Fermi surface. The instanton size was fixed at $\rho p_F = 1$, corresponding to $\rho = 0.4, 0.2, 0.1$ fm.

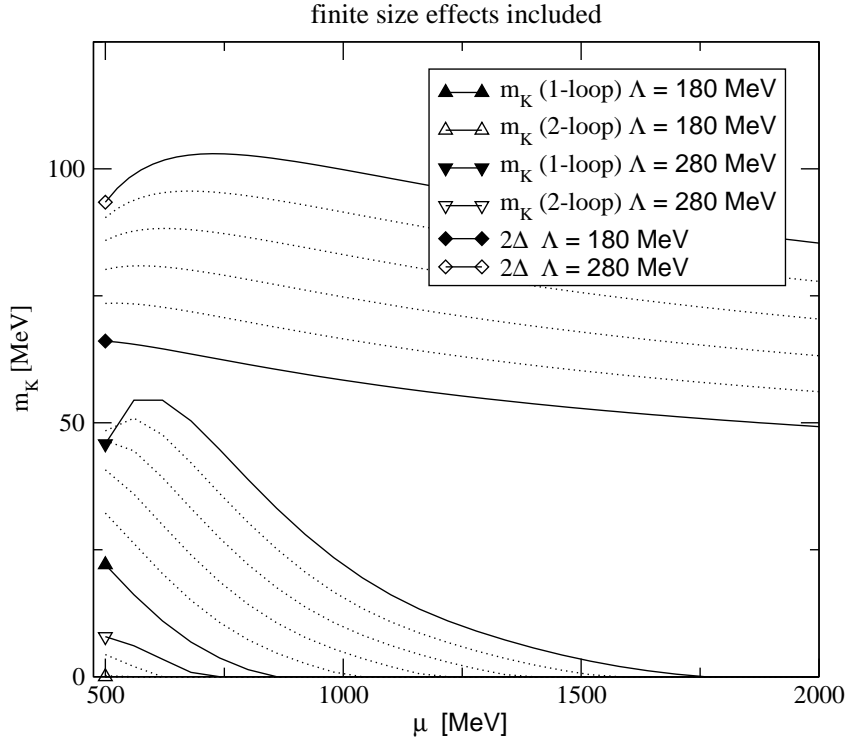


FIG. 6. Same as Fig. 3 but with instanton finite size effects (instanton form factors) included.

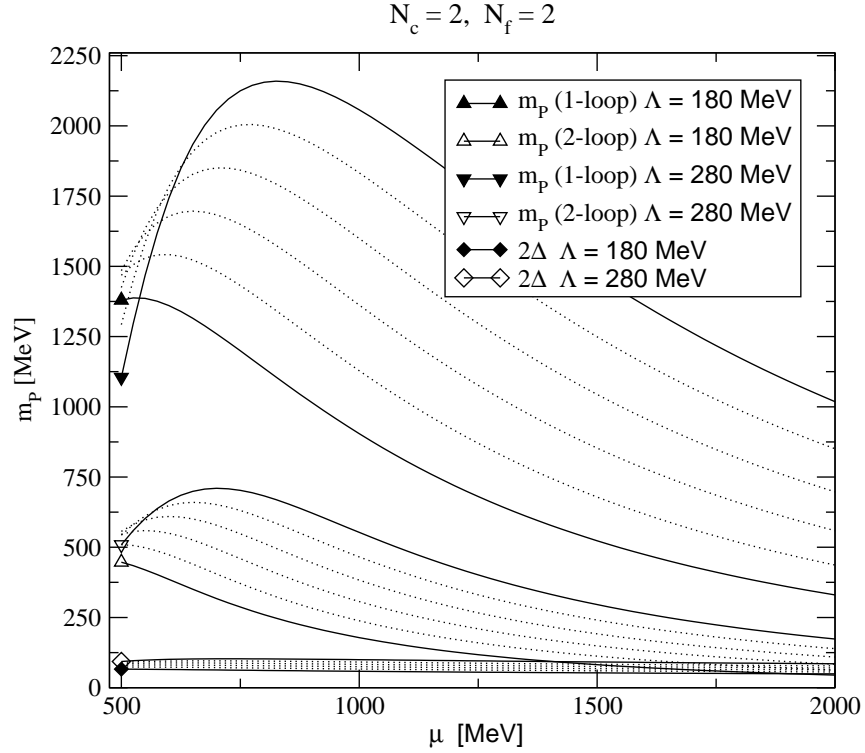


FIG. 7. Pseudoscalar Goldstone boson mass in $N_c = 2$ QCD. The two sets of curves correspond to the one and two-loop instanton size distribution and different values of the scale parameter, see Fig. 2. For comparison, we also show the energy gap 2Δ .

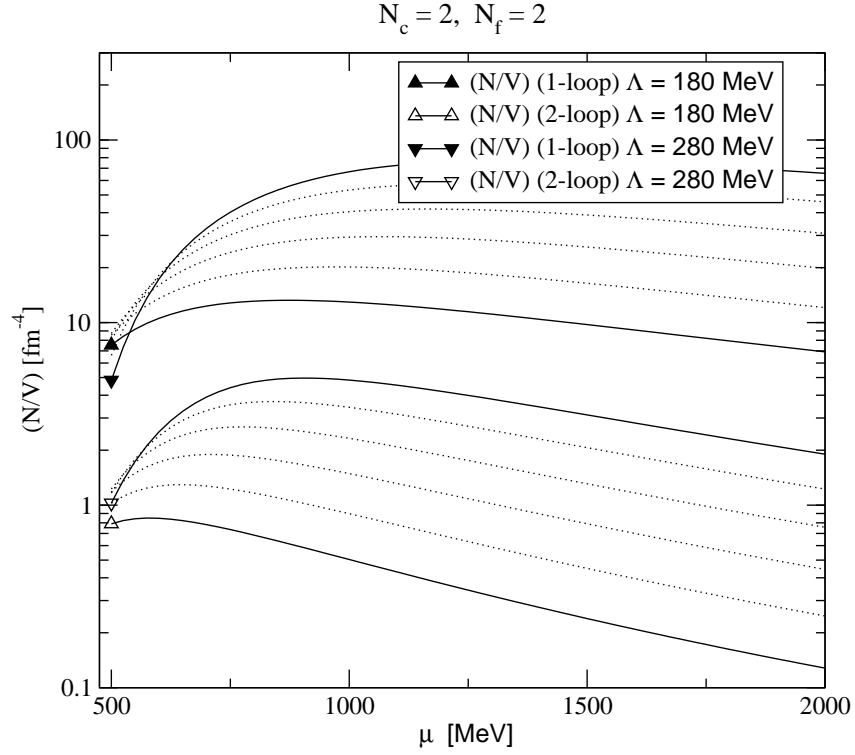


FIG. 8. Instanton density in $N_c = 2$ QCD. The two sets of curves correspond to the one and two-loop instanton size distribution and different values of the scale parameter in the range $\Lambda = (180 - 280) \text{ MeV}$.